Reversible Alteration of Morphology in an Invertebrate Erythrocyte: Properties of the Natural Inducer and the Cellular Response

CHRISTINE LEMA-FOLEY, KYENG G. LEE, TCHAIKO PARRIS, ZOYA KOROLEVA,
NISHAL MOHAN, PIERRE NOAILLES, AND WILLIAM D. COHEN*

*Department of Biological Sciences, Hunter College of CUNY, 695 Park Ave., New York, New York
10021; and Marine Biological Laboratory, Woods Hole, Massachusetts 02543*

Abstract. The normal shape of the erythrocytes of the bivalves known as *blood clams* is maintained by a marginal band (MB) of microtubules. When hemolymph (or "blood") is withdrawn from the animal, its erythrocytes change, within minutes, from the normal smooth-surfaced, flattened ellipsoids (N-cells) to spheroids with folded surfaces (X-cells). This alteration can be prevented by rapidly diluting the hemolymph with physiological medium, yielding N-cells for use in studying the transformation to X-cells. Bioassays showed that shape transformation was induced by a hemolymph activity (H_x) and was a function, in part, of cell responsiveness to this activity. Eventually the shape of the cells spontaneously returned to normal, at a rate dependent upon the concentration of the cells and of H_x; recovery was correlated with loss of H_x. The X-cells contained an intact but highly deformed MB, but this was not the effector of the transformation. Erythrocytes made to lack MBs still changed shape, although they did not recover as completely as did the MB-containing controls. When clams were cooled before hemolymph was withdrawn, the concentration of H_x was reduced. H_x was retained after dialysis of hemolymph, and initial filtration and chromatography indicated that its M_r was greater than 500,000. Shape transformation was blocked by EGTA, by serine protease inhibitors, and by sodium azide; the last indicates ATP-dependence. Although the mechanism responsible for shape transformation remains to be determined, the data suggest that the change is triggered by a coagulation-related activity in response to the removal of hemolymph from the animal.

Introduction

The nucleated erythrocytes of non-mammalian vertebrates are useful for studying the role of cytoskeletal elements in cellular morphogenesis and cell-shape maintenance. When mature, these cells are characteristically flattened ellipsoids or discoids with a nuclear bulge. Their cytoskeletal system contains a marginal band (MB), composed principally of microtubules, enclosed within the membrane skeleton (MS) in the plane of flattening, and in at least some species, intermediate filaments link sites on the MS to the MS or nucleus. The morphology of these cells is relatively stable and is maintained by the MB against potentially deforming mechanical or osmotic forces (Joseph-Silverstein and Cohen, 1984, 1985; Cohen, 1991). Certain invertebrates also have hemoglobin-bearing nucleated erythrocytes (Ratcliffe and Rowley, 1981; Cohen and Nemhauser, 1985), and in some cases these cells change morphologically when they are removed from the animal (*e.g.,* Terwilliger *et al.,* 1985). Erythrocyte-containing species include bivalves of the genera *Anadara* and *Noetia*. The cytoskeletal system of their red cells resembles that of non-mammalian vertebrates but, unlike the latter, it also includes a functional centrosome associated with the MB (Cohen and Nemhauser, 1980; Nemhauser *et al.,* 1983). Most importantly for the present work, the shape of the erythrocytes changes drastically—from normal flattened ellipsoids ("N-cells") to wrinkled spheroids ("X-cells")—in hemolymph samples from these and related species (Sullivan, 1961; Cohen *et al.,* 1985). We have found that this transformation is induced by a hemolymph activity, and that, surprisingly, it eventually reverses spontaneously, so that the cells return to a near-normal shape ("R-cells";

Dadacay *et al.*, 1996). This is the only natural, reversible morphological change in non-mammalian erythrocytes of which we are aware, and it offers an opportunity to analyze the interplay between extracellular factors and cytoskeletal elements in maintaining cellular shape. We present here experimental work that defines major properties of the natural inducing factors and of the cellular response in this system.

Materials and Methods

Experimental material

Specimens of *Noetia ponderosa* (the "ponderous ark") were obtained from Terry Bros. Co. (Willis Wharf, VA) and were maintained in a refrigerated seawater tank at about 17°C or in the running natural seawater system at the Marine Biological Laboratory. Blood from the mantle cavity or foot muscle was drawn using syringes with 22- or 27-gauge needles, or was obtained by cutting muscle during clam sacrifice. Shape-transforming activity in the whole blood, as measured by the percentage of X-cells present, was recorded 5 or 10 min after blood was obtained, when it was typically maximal. Because we occasionally found clams in which activity was very low, we adopted an activity of 85% or greater as the minimal level for subsequent experimental use.

To obtain N-cells (cells of normal morphology that had not undergone transformation), blood was immediately diluted a minimum of 1:200 into "physiological medium" consisting of MBL formula artificial seawater (Cohen, 1997) containing 0.5 m*M* NaH$_2$PO$_4$ at pH 7.2, in which cells retained normal shape. In a few experiments, marine molluscan Ringer's solution (MMo-1; Cohen, 1997), a similar medium also containing 0.5 m*M* NaH$_2$PO$_4$ at pH 7.2, was employed with the same results. The resulting suspension was centrifuged (2000 rpm, 3 min, Beckman Accuspin at 17°C), yielding an erythrocyte pellet overlaid by a thin layer of white cells and trapped erythrocytes. This layer was removed by aspiration, and the cells were washed two or three times by centrifugation in about 5 times the original blood volume of physiological medium. Washed erythrocytes were resuspended to the original blood volume and hematocrit was measured to determine cell concentration by volume. N-cells were ready for use after final adjustment to a concentration of 1% by volume and inspection with phase contrast microscopy to verify normal shape.

Bioassay of shape transforming activity

Cell-free hemolymph was obtained as the supernate after a 3-min microfuge centrifugation of whole blood. As noted previously (Dadacay *et al.*, 1996), the shape-transforming activity (H$_x$) of cell-free hemolymph was stable with freezing, permitting storage of hemolymph at −20°C or −80°C

until use. The basic bioassay consisted of suspending N-cells in normal or experimentally treated cell-free hemolymph (*t* = 0), incubating at 21°–23°C (room temperature), then counting samples under phase contrast to determine the percentage of X-cells present after 5 min and at subsequent time points. Samples were either counted rapidly, to avoid appearance of morphology-distorting "glass effects," or were fixed in physiological medium containing 8% formaldehyde before counting. In each sample (*i.e.*, per data point), 200 or more cells were counted in non-selected fields. Unless otherwise specified, cell-free hemolymph was diluted with physiological medium just prior to use, such that the X-cell concentration reached 90% or more within 5–10 min, and reversal to less than 10% X-cells occurred in 1–2 h.

Experiments involving bioassays were performed a minimum of three times using material from different clams, unless otherwise noted; each data point records a specific cell count, and the data presented are representative.

Preparation of erythrocytes with and without marginal bands

Erythrocytes were pre-incubated with either no inhibitor (dimethyl sulfoxide [DMSO] solvent only), 10 µg/ml nocodazole, or 20 µ*M* taxol (Sigma Chemical Co., St. Louis, MO) for 30 min at room temp. (22°–24°C) and subsequently incubated at 0°C for 3 h. These cell suspensions (still containing inhibitors) were then rewarmed for 30 min at room temperature (22°–24°C), and the presence or absence of MBs was ascertained by phase-contrast examination of cytoskeletons produced in Triton lysis medium. Triton lysis medium consisted of 100 m*M* piperazine-*N*,*N*'-bis(ethanesulfonic acid) [PIPES buffer], 5 m*M* ethylene glycol-bis-(β-aminoethyl ether) *N*,*N*'-tetraacetic acid [EGTA], 1 m*M* MgCl$_2$, pH 6.8 (=PEM), containing 0.4% Triton X-100 (Cohen and Nemhauser, 1980, 1985; Joseph-Silverstein and Cohen, 1984). MBs were observed in taxol-treated or untreated cells, but were not present in nocodazole-treated cells (Joseph-Silverstein and Cohen, 1984, 1985).

Microscopy

Cells for morphological examination were either unfixed or fixed immediately (<30 s) by dilution into physiological medium containing 4%–8% formaldehyde. Cells were examined and images recorded using a Zeiss phase contrast microscope equipped in most instances with a DAGE NC-70 video camera, Hamamatsu Argus-10 video image processor, and video printer.

For fluorescence microscopy, living cells suspended in physiological medium were first trapped within fibrin clots as described previously (Lee *et al.*, 1998; see also Forer and Behnke, 1972). Briefly, 1 volume of cell suspension was mixed with 4 volumes of the same medium containing
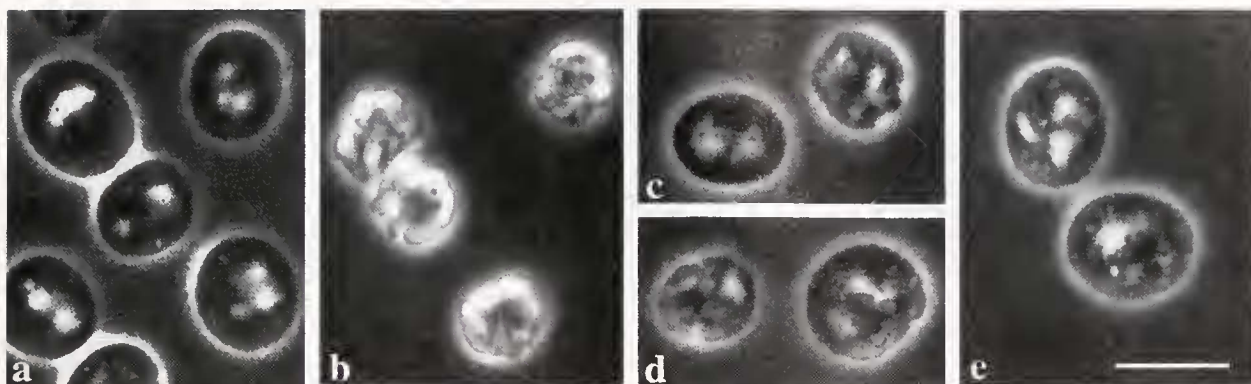
Figure 1. Light micrographs of *Noetia ponderosa* erythrocytes before and after shape transformation. (a) Normal erythrocytes (N-cells), flattened and slightly ellipsoidal; (b) shape-transformed erythrocytes (X-cells), appearing refractile, lumpy, and spheroidal at this level of resolution; (c, d) examples of shape-transformed erythrocytes at different stages during recovery; (e) cells of essentially normal shape post-recovery. Video-enhanced phase contrast microscopy; bar = 10 μm.

10 mg/ml fibrinogen (Sigma F-8630). Thrombin (Sigma T-4648) was added to 1 U/ml to produce a firm clot in about 10 min; within this time window, 5- to 25-μl samples were spread inside plastic rings adhering to coverslips. Cytoskeletons were produced by immersing coverslips bearing fibrin-trapped cells in Triton lysis medium (see above) for 1 min, followed by fixation in PEM containing 8% formaldehyde. In some cases, 4% formaldehyde was included in the lysis medium for additional stabilization. This was followed by PBS washes and incubation with a 50:50 mix of monoclonal anti-α- and anti-β-tubulin (Sigma T-9026, T-4026), using secondary FITC goat anti-mouse IgG F(ab')$_2$ (Sigma F-8521). Fibrin-trapped specimens were examined using epifluorescence and confocal fluorescence microscopy. Controls lacking primary antibody or phalloidin exhibited little background fluorescence.

For scanning electron microscopy, cells were fixed for 1 h in 16% formaldehyde in 0.5 M KH$_2$PO$_4$, pH 6.8, at 21°–23°C (room temperature); dehydrated in ethanol to 70%; incubated on acid-cleaned polylysine-coated coverslips; dehydrated to 100% ethanol; and critical-point dried (Tousimis Samdri-780A). Coverslips were mounted on stubs with double-sided tape and sputter coated with Au/Pd (Tousimis Samsputter 2A), with silver paste added for conductivity.

Hemolymph dialysis, filtration, and chromatography

Hemolymph samples were dialyzed overnight at 0°C against physiological medium in dialysis tubing with a molecular weight cutoff of about 12,000; control samples were similarly treated except that the dialysis medium was omitted. Hemolymph fractions were obtained by centrifugation through Centricon concentrators (Amicon Inc.) of various molecular weight cutoffs (10,000–500,000), and by chromatography on Sephadex G-200SF and Sephacryl

400HR columns. The protein content of the fractions was assayed by the Bradford method (Bradford, 1976), and fractions were bioassayed for H$_x$ as described above.

Results

Cell morphology

As observed by video-enhanced phase contrast of fixed samples, normal erythrocytes ("N-cells") were flattened ellipsoids when initially removed from the animal (Fig. 1a). Upon incubation in cell-free hemolymph under our standard assay conditions, most N-cells were transformed to an irregular spheroidal shape (X-cells) within 5–10 min (Fig. 1b), with a lag of several minutes, but eventually recovered normal or near-normal shape ("R-cells"; Fig. 1c–e).

More detailed views of cell morphology were obtained by scanning electron microscopy. Surveys at lower magnifications verified the light microscopic observations (Fig. 2). At higher magnifications it was clear that N-cells were relatively smooth-surfaced (Fig. 3a, b), whereas the surface of X-cells was thrown into large folds (Fig. 3c, d).

Shape transformation: time course and general features

In undiluted hemolymph, recovery of most of the erythrocyte population typically required many hours. In hemolymph diluted in the range of ½ to ⅕ with physiological medium, time spent in the fully transformed state was progressively reduced. A typical time course for shape transformation and recovery in diluted hemolymph is presented in Figure 4, and a comparison of cell response to undiluted and diluted hemolymph is shown in Fig. 5. The rate of shape reversal was positively correlated with erythrocyte concentration (Fig. 6).

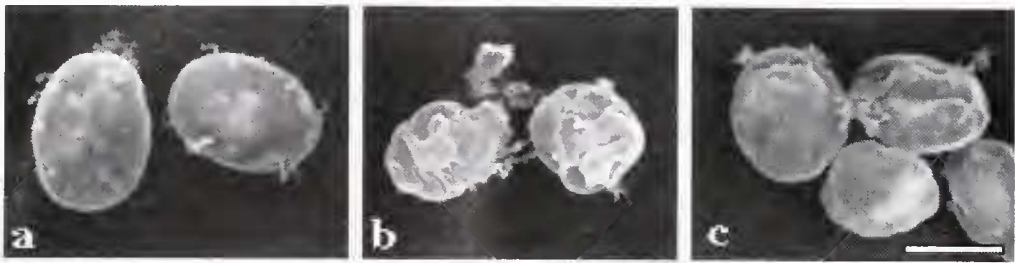Shape transformation was not triggered by a change in hemolymph pH, nor could it be mimicked by simple

Figure 2. Survey view of *Noetia ponderosa* erythrocytes. (a) Normal cells, flattened and ellipsoidal; (b) shape-transformed erythrocytes; (c) erythrocytes during recovery. Scanning electron microscopy; bar = 10 μm.

changes of pH in the medium. Cells were found to be morphologically stable over a tested pH range of 6.6–7.5 in physiological medium, and the pH of native cell-free hemolymph remained stable at about 6.7 as measured before and after shape transformation.

Cell responsiveness

The percentage of cells that changed shape was markedly lower in native blood samples from certain clams. To test whether this was due to variable H_x or to variable cell
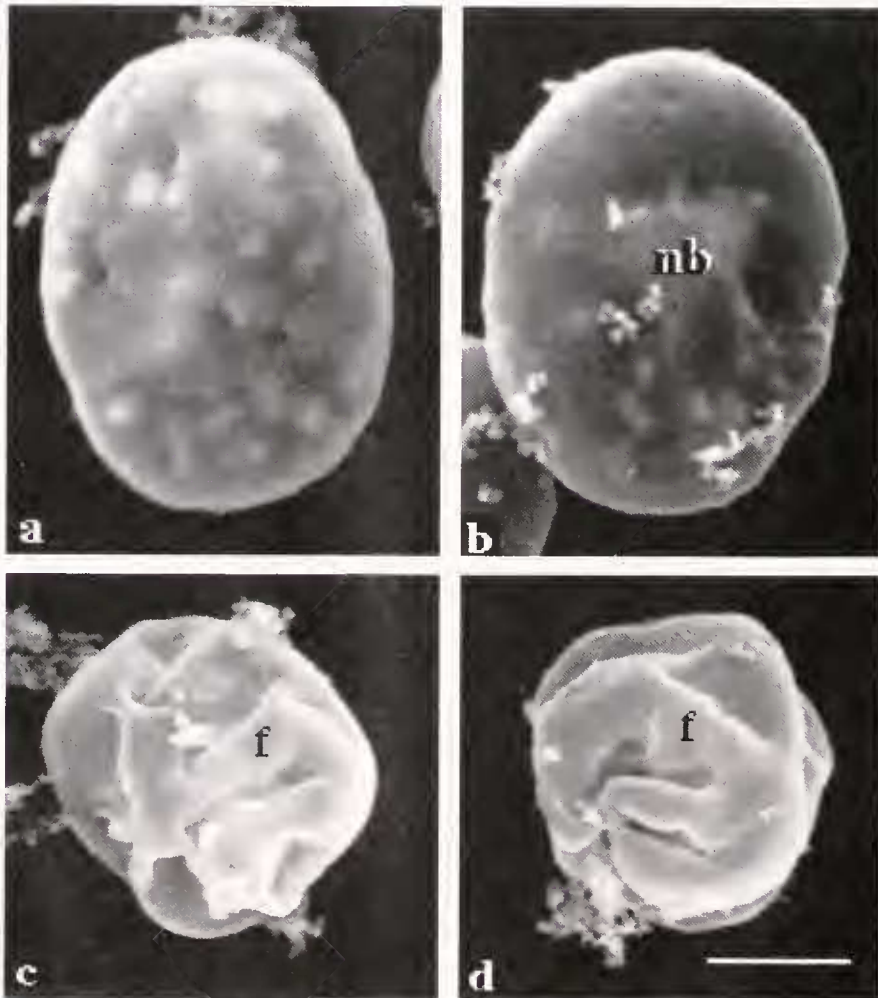

Figure 3. Higher magnification view of two cells in Figure 2, plus two additional examples: (a, b) Normal erythrocytes, flattened and ellipsoidal (nb = nuclear bulge); (b) shape-transformed erythrocytes, with "lumpiness" resolved as extensive surface folding. Scanning electron microscopy; bar = 10 μm.
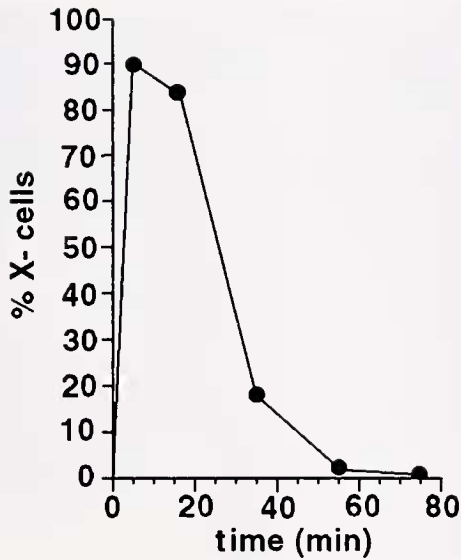
Figure 4. Typical time-course of cell-shape transformation and recovery in diluted hemolymph. The percentage of X-cells rose to >90% within 5 min, held at >80% for ~15 min, and declined to near zero by 60 min.

responsiveness to H_x. N-cells and hemolymph were prepared from clams exhibiting high and low levels of native shape transformation respectively, and cells and hemolymph were mixed in all four combinations. The results (Fig. 7) show that H_x was high in all hemolymphs, but that erythrocytes of two different clams can vary greatly in their responsiveness to hemolymph from the same clam.

Figure 6. Effect of cell concentration on cell-shape transformation and recovery (undiluted hemolymph). At the standard cell concentration (1%) the percentage of shape transformation was maximal, with only modest subsequent reversal. At higher cell concentrations the peak percentage of X-cells was reduced, and reversal rate was progressively greater.

Post-recovery cell responsiveness and depletion of Hx

Cells that had recovered normal shape (R-cells) were able to undergo a second transformation to X-cells, comparable to that of controls, when transferred into fresh hemolymph
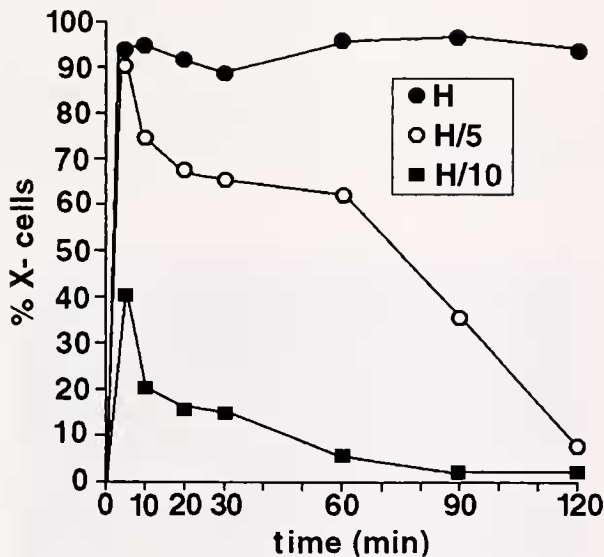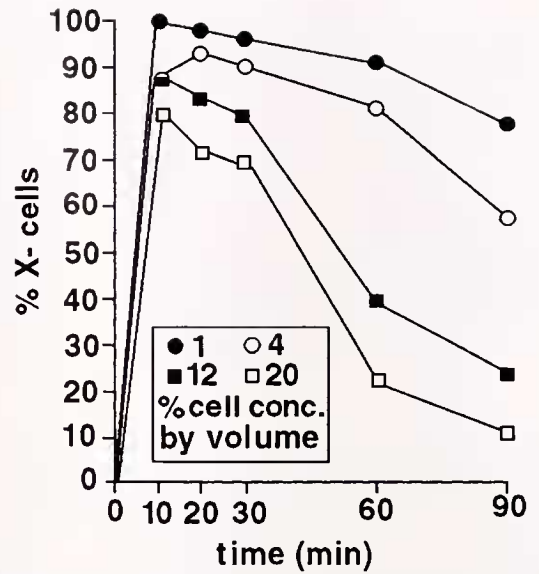

Figure 5. Effect of hemolymph dilution on cell-shape transformation and recovery. H = undiluted hemolymph; H/5 and H/10 = hemolymph diluted 1:5 and 1:10 with physiological saline, respectively. Note that <50% of the cells responded in H/10. In experiments such as this using undiluted hemolymph, reversal to <10% X-cells was frequently not observed for 6 or more hours.
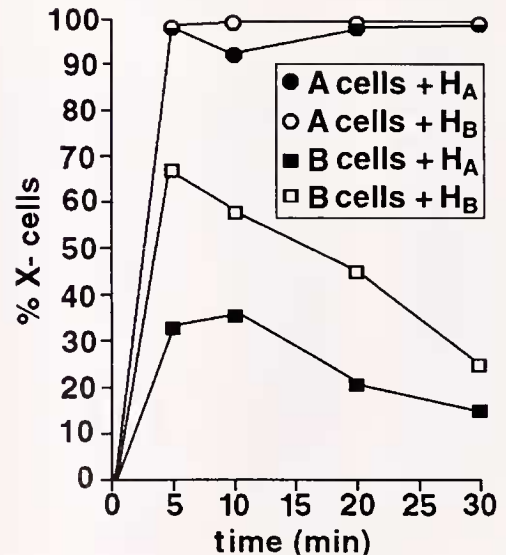

Figure 7. Dependence of shape transformation on cellular factors. Cells and cell-free hemolymph (H) were obtained from two clams (A and B), and all four mixtures were made as indicated. Clam A cells yielded >90% X-cells within 5 min and maintained that activity independent of hemolymph source, whereas clam B cells showed submaximal activity independent of hemolymph source.
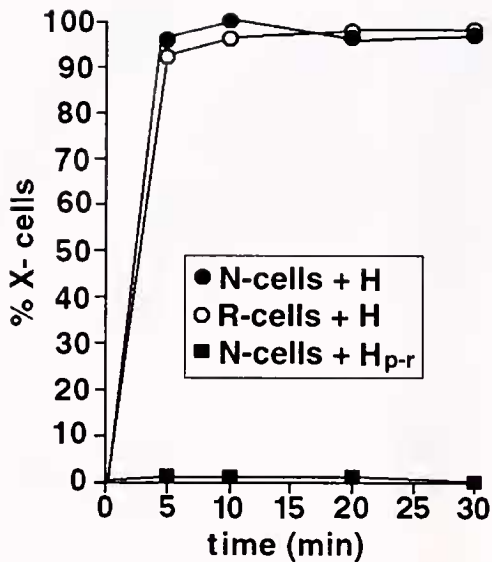
Figure 8. Assay for hemolymph activity (H$_x$) following cell-shape transformation and recovery, and test of capacity of recovered cells (C$_R$) to undergo a second transformation. Upon recovery, R-cells reincubated with fresh hemolymph again underwent shape transformation, whereas reincubation of fresh N-cells in the "post-reversal" cell-free hemolymph (H$_{p-r}$) showed that it lacked H$_x$.
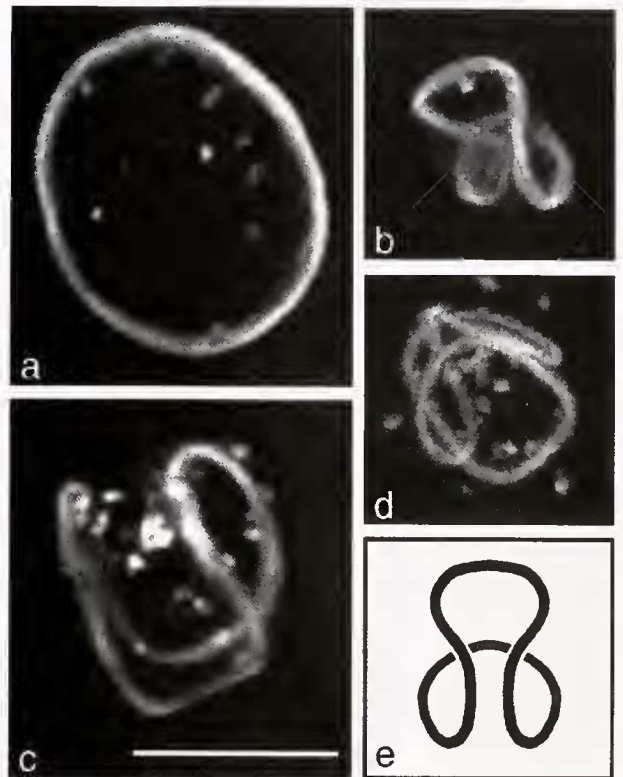

Figure 9. Marginal bands (MBs) of microtubules as revealed by anti-tubulin immunofluorescence. (a) N-cell cytoskeleton; (b–d) X-cell cytoskeletons. N-cell MBs were typically ellipsoids, sometimes twisted into figure-8s. X-cell MBs were essentially intact, but assumed highly convoluted shapes without apparent breakage. A diagram of the basic MB deformation pattern observed in many X-cells (*e.g.,* b, c) is given in (e); some twist patterns were more complex, however (*e.g.,* d). Fluorescence microscopy; bar = 10 μm.

(Fig. 8, open circles). However, the converse was not true: N-cells incubated in hemolymph in which other cells had previously undergone shape transformation and recovery either remained normal or exhibited only partial transformation and very rapid recovery, indicating depletion of H$_x$ (Fig. 8, squares).

Cytoskeletal structure and function

As revealed by indirect anti-tubulin immunofluorescence, the MB was still present and continuous in the cytoskeletons of shape-transformed cells, but its shape was highly convoluted compared to that of normal cells (Fig. 9). To test whether the MB was a primary effector of shape transformation, erythrocytes with and without MBs were prepared by temperature cycling in the presence of inhibitors of disassembly (taxol) or reassembly (nocodazole). Similarly cycled controls (DMSO solvent only) contained completely or partially reassembled MBs. Bioassays in diluted hemolymph produced more than 96% X-cells in all three preparations within 10 min, and reversal after 3 h.

One major difference was noted in cells lacking MBs, however: many of the major transformation-induced surface indentations were not eliminated during reversal (Fig. 10).

Shape transformation inhibitors

Heating hemolymph in a boiling water bath, followed by cooling and bioassay, showed H$_x$ to be heat-labile. In three experiments in which controls showed very high initial

activity (99% at 10 min), samples heated for 20 min exhibited initial residual activity of 75%–95%, but recovery of cell shape began after only about 20 min. By 60 min, experimentals had 0%–15% X-cells, whereas controls still
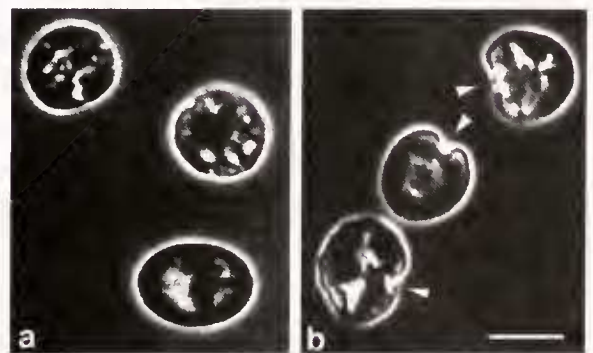

Figure 10. Shape reversal in cells containing or lacking MBs. (a) MB-containing cells; only minor post-reversal surface deformations were observed; (b) cells lacking MBs; major surface indentations were retained post-reversal. Video-enhanced phase contrast microscopy; bar = 10 μm.
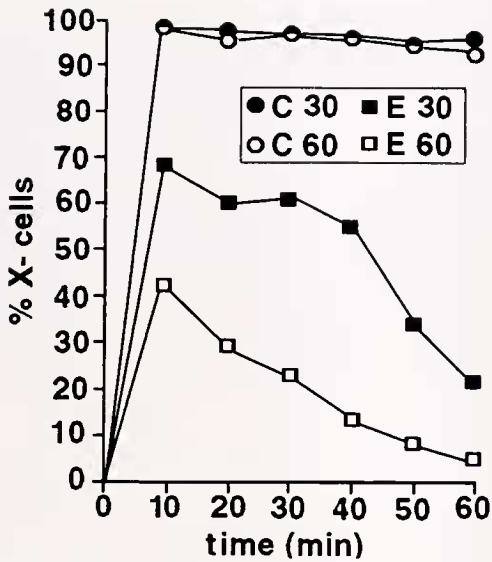
Figure 11. Effect of sodium azide on shape transformation and recovery. N-cells were incubated for 30 or 60 min in 3 mM sodium azide in physiological medium (=experimentals E30 and E60) or in physiological medium alone (=controls C30 and C60) prior to assay. Azide pre-incubation markedly reduced the percentage of X-cells and accelerated shape reversal, with greater effect for the 60-min period. Controls maintained >90% X-cells throughout.

had 95%–99%. In two additional experiments, controls with 90%–93% initial activity retained 80%–90% after 30 min, whereas experimentals heated for 10 min had only 5%–6% X-cells initially, and less than 2% in 30 min.

Bioassays were conducted with various potential biochemical inhibitors added to hemolymph prior to the addition of N-cells. Shape transformation was completely inhibited by 10 mM (or greater) EGTA, as reported previously (Dadacay *et al.*, 1996); at a given concentration, EDTA was less effective. The protease inhibitors initially surveyed were antipain, aprotinin, bestatin, chymostatin, leupeptin, aminoethylbenzenesulfonyl fluoride (AEBSF), and phosphoramidon. As assayed after a 10-min exposure, only chymostatin and AEBSF were effective, at 18% and 7% X-cells, respectively (*vs.* 91% for controls). AEBSF produced complete inhibition at 3 mg/ml (12 mM) and above, and an excess (5 mg/ml) was typically employed in other experiments.

ATP-dependence of shape transformation was tested by pre-incubation of N-cells in physiological medium containing 3 mM sodium azide for either 30 min or 60 min, followed by a wash, prior to mixing cells and cell-free hemolymph. Controls were similarly incubated, except without azide. As shown in Figure 11, the percentage of cells undergoing shape transformation was markedly reduced and shape reversal accelerated in both cases compared to controls, with the longer period of ATP depletion having the greater effect.

Activity sequence

The inhibitor studies indicated that shape transformation involved a calcium-activated step and a proteolytic activity, but in what sequence did they occur? To answer this question, N-cells were mixed with hemolymph at $t = 0$, and inhibitors were added at subsequent time intervals (Fig. 12). EGTA was found to be effective only if present initially ($t = 0$); in contrast, AEBSF was effective initially and was at least partially effective at later time points. Importantly, when added at $t = 5$ min and 10 min, AEBSF induced some shape reversal, whereas EGTA did not.

Triggering of transformation activity

Shape transformation was apparently triggered during the removal of blood and thus might be a response to wounding. Three pairs of clams were used to test this hypothesis: physiological responsiveness was reduced by pre-cooling clams to 1°C, and tissue trauma was minimized by removing blood through a very fine (28-ga) syringe needle. The activity of hemolymph obtained using both variables together (assayed using N-cells from a non-cooled clam) was reduced to about 50% of that of hemolymph obtained from the same clam after re-warming and sacrifice by slashing muscle (Fig. 13). Activity reduction of lesser extent was also observed when each variable was tested separately (low temp. *vs.* normal; fine needle *vs.* sacrifice; not shown).
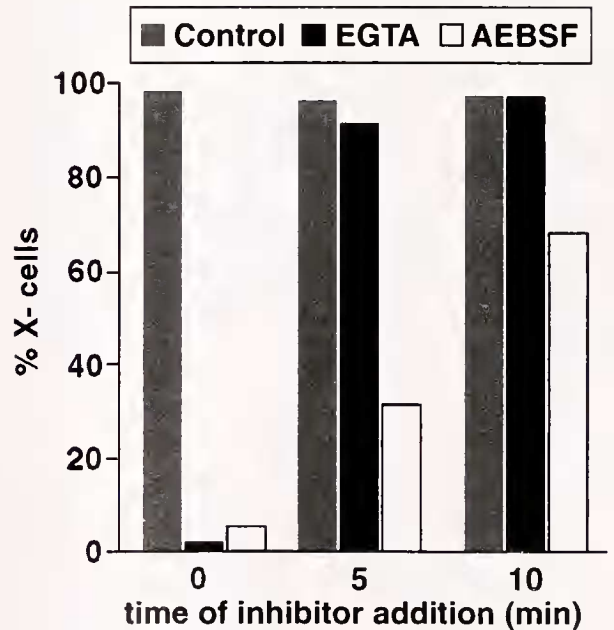

Figure 12. Effect of addition of EGTA and AEBSF at various times after exposure of N-cells to hemolymph. The percentage of X-cells was determined 5 min after the addition of inhibitor (final concentrations: 20 mM EGTA, 5 mg/ml AEBSF). EGTA was effective only when present initially, whereas AEBSF was still partially effective when added later.
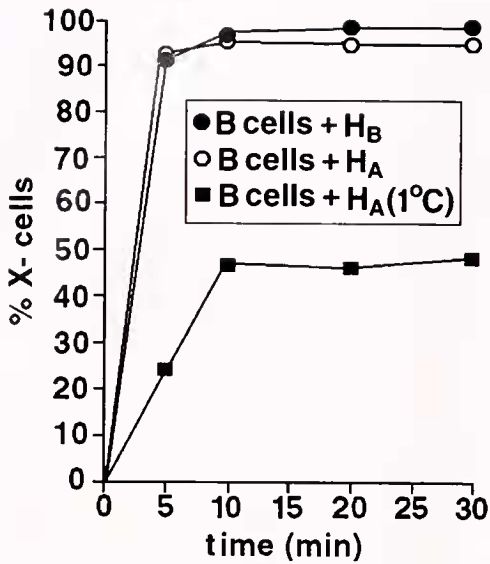
Figure 13. Tissue trauma as a possible factor in H_x level. Two preparations of cell-free hemolymph were made from clam A: $H_{A(1°C)}$ was obtained *via* syringe after pre-cooling clam A to 1°C, and H_A from the same clam was obtained by cutting muscle after 3 h of rewarming. N-cells (C_B) and cell-free hemolymph for control bioassay were obtained from clam B. Three mixtures were made as indicated, with $H_{A(1°C)}$ exhibiting less than half the activity of H_A.

Dialysis and initial fractionation of hemolymph

Active hemolymph was dialyzed for 12 h against physiological medium at 0°C, with a molecular weight cutoff of about 12,000. Control hemolymph was similarly treated except that the dialysis sac was simply kept moist. Bioassay with fresh N-cells showed that both samples exhibited excellent activity, with the experimental comparable to the control except for an extended activation lag (Fig. 14). Centrifugation through filters with different molecular weight cutoffs (Centricon) indicated that the M_r for H_x is greater than 500,000, and chromatogaphy on Sephadex G-200SF confirmed that H_x moved together with the blue dextran marker, indicating the M_r to be greater than 250,000.

Discussion

Shape transformation and recovery

The results show that shape transformation occurs in response to an activity (H_x) in the cell-free hemolymph, and that the extent of response is a property of the erythrocyte population. In typical assays, more than 90% of cells were responsive to H_x, but individual cells, as well as cells from certain clams, varied in both responsiveness and rate of recovery. Variability was particularly clear at high hemolymph dilutions (*e.g.*, Fig. 5, H/10), in which only a fraction of the erythrocytes responded. This was verified by experiments using erythrocytes from clams with high *vs.* low percentages of transformation, in which the variable response was attributable to cells rather than hemolymph (Fig. 7). In addition, recovery during a typical time course (*e.g.*, Figs. 4–6) was not synchronous, indicating a range of cell sensitivity to H_x.

Cells that had undergone shape transformation and recovery (R-cells) retained the capacity to change shape a second time (Fig. 8). In contrast, hemolymph assayed after removal of R-cells was depleted of H_x, and thus the recovery phenomenon is correlated with loss of H_x. The increased rate of recovery with increasing cell concentrations (Fig. 6) is consistent with increased cell-induced loss of H_x.

Biochemical activities involved in shape transformation

Shape transformation was markedly inhibited by EGTA, with EDTA less effective, indicating that the process is Ca^{++}-activated. Transformation was also greatly reduced by preheating of hemolymph and blocked by the serine protease inhibitors AEBSF and chymostatin. Both EGTA and AEBSF were effective when present at $t = 0$ (mixing of N-cells and hemolymph), but only AEBSF was effective when added later (Fig. 12). Thus, the initial step is presumed to be Ca^{++}-activated, resulting in a hemolymph proteolytic activity for which Ca^{++} is no longer required.

One relatively simple hypothesis is that a proteolytic product maintains cell shape transformation, and that cells recover when the proteolytic activity ceases and product concentration falls. This is at least partly supported by the observation that addition of AEBSF produces considerable reduction in the percentage of X-cells present (Fig. 12)
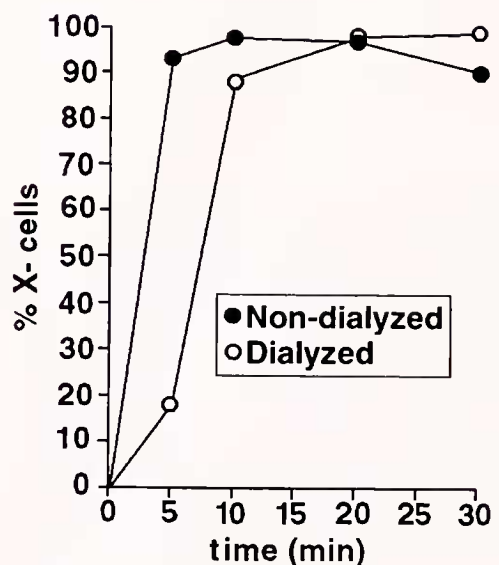

Figure 14. Activity of cell-free hemolymph after dialysis. Non-dialyzed and dialyzed hemolymph reached comparable X-cell levels, with the latter exhibiting a longer lag period.

compared to controls. With time, the X-cells presumably inhibit this proteolytic activity or exhaust its product, accounting for the loss of transforming activity in post-recovery hemolymph.

Mechanism of shape transformation and recovery

ATP-depletion by pre-incubating the erythrocytes with azide inhibits shape transformation in most of the cell population, showing that it is an active phenomenon. Three hypotheses for an active shape-transformation mechanism are (a) alteration of MB shape by a microtubule-motor protein system, (b) contraction of a cell-surface–associated actomyosin system, and (c) reduction of cell volume by an osmotic pump system. Each is considered here in relation to the data.

(a) Microtubule-motor protein mechanism: MB function. Transformation of cell shape, as well as initiation of shape reversal, takes place in the presence or absence of the MB; thus, the MB is not the primary effector, and this mechanism can be ruled out. However, the MB is needed to return to completely normal cell shape (Fig. 10), a finding consistent with previous studies showing that the MB is required for the erythrocytes of dogfish and blood clams to resist deformation caused by mechanical and osmotic stress (Joseph-Silverstein and Cohen, 1984, 1985).

Whereas normally the MB of the blood clam erythrocyte appears to deform the MS and maintain its shape (Joseph-Silverstein and Cohen, 1985), the mechanism at work here generates sufficient force to produce substantial secondary deformation of the MB (Fig. 9b–d). Such deformation without breakage demonstrates that the MB has remarkable flexibility, as expected for shape-maintenance function. The contours assumed by many of these deformed MBs appear to be twisted variations of a "baseball seam" model, in which a spheroidal shape is accommodated by an initially planar ellipse folding back on itself (Fig. 9e). The complete cell-shape recovery observed in the presence of azide is compatible with non-ATP-requiring, mechanical MB function in response to deformation.

(b) Cell-surface–associated actomyosin contraction mechanism. The entire X-cell surface has a folded appearance, and thus the underlying membrane skeleton (MS) is a potential cytoskeletal effector. We have observed previously that F-actin is prominently associated with the *Noetia* erythrocyte MS (Lee *et al.*, 1998), but the presence of myosin has not yet been demonstrated in these cells. Myosin resembling that of platelets has, however, been identified in mammalian erythrocytes (Fowler *et al.*, 1985). It can form bipolar filaments (myosin II class) and is believed to participate in contractile activity associated with the erythrocyte membrane (Fowler, 1986; Pasternack and Racusen, 1989; der Terrossian *et al.*, 1994). Thus there is sufficient

precedent for serious consideration of such a mechanism in blood clam erythrocytes.

(c) Active reduction of cell volume by osmotic efflux. The appearance of shape-transformed cells (Fig. 3) is compatible with osmotic distortion, and osmotic mechanisms are attractive in being potentially readily reversible. However, if an osmotic mechanism is at work here, it cannot be a simple phenomenon attributable to use of physiological media or other experimental manipulations. First, the native shape of these red cells is flattened and ellipsoidal, as shown previously by immediate fixation of blood samples (Cohen and Nemhauser, 1986); when the "blood" is diluted immediately and extensively with our physiological media, the cells retain their native shape indefinitely. Second, both the shape change and recovery occur in the clam's own hemolymph without any experimental manipulation whatever. Third, hemolymph diluted tenfold with physiological medium in which N-cells are osmotically stable still induces complete shape change in some cells of the population. Fourth, freshly added N-cells are morphologically stable in hemolymph in which cells have undergone the complete cycle of transformation and recovery (Fig. 8). Finally, the effect cannot be mimicked by suspension of N-cells in hyperosmotic media, as reported earlier (Dadacay *et al.*, 1996); N-cells get thinner in such media, but retain their flattened ellipsoidal shape.

It is quite possible, however, that the shape transformation involves a more complex osmotic mechanism, such as one in which an external signal triggers hyperactivity of an active efflux system that produces and maintains excessive volume loss until reversal. Amende and Pierce (1980a) have shown that hypo-osmotically stressed *Noetia* red cells reduce their volume to normal levels by a mechanism involving active efflux of taurine and other amino acids. Like the shape transformation reported here, this osmoregulatory mechanism is activated by Ca^{++} and inhibited by ATP depletion (Amende and Pierce, 1980b; Pierce and Maugel, 1985; Pierce *et al.*, 1989). Thus it is possible that activation of the same system in N-cells by some other means could further reduce cell volume. We have not reported hematocrit volume measurements in this paper, however, because we believe that differences in the packing of N-cells—smooth-surfaced, flattened ellipsoids—and X-cells—spheroids with highly folded surfaces—make such data highly unreliable. Studies of this mechanism will require more sophisticated volume measurements.

Triggering of erythrocyte shape transformation

The hemolymph of this and closely related molluscan species (*Anadara ovalis, A. transversa*) does not undergo complete *in vitro* clotting in the classic sense, but microscopy of whole-blood samples shows that white hemocytes begin to aggregate shortly after the blood is obtained. In

other molluscs (oysters, mussels), hemocytes have been shown to aggregate at wound sites and plug them (Sparks and Morado, 1988), and eventual spontaneous disaggregation has also been observed in oysters under certain conditions (Bang, 1961; Feng, 1965, 1988). The act of obtaining hemolymph by syringe or by tissue cutting may initiate similar wound-repair mechanisms in blood clams, with elevation of Ca^{++} by entry of seawater a possible trigger. Erythrocyte shape transformation might then be a secondary effect triggered and maintained by a local mechanism of wound repair, with recovery advantageous for affected erythrocytes that move away from the site and enter the general circulation.

The data are consistent with the idea that the mechanism for triggering shape alteration is analogous to that of vertebrate blood clotting, in which Ca^{++} is required for early activation steps, serine protease activity yields fibrin, and generation of plasmin causes clot dissolution (reversal). The analogy is not necessarily superficial, as serine proteases are involved in clotting cascades in certain other invertebrates (e.g., Limulus; Bergner et al., 1997). Though not the focus of present work, initial characterization of molecular species participating in H_x showed retention of activity in dialyzed cell-free hemolymph, indicating that components of relatively low molecular mass ($<12,000$ Da) were not involved. H_x was present in fractions produced by column chromatography and centrifugal filtration that respectively indicate M_r values of more than 250,000 and more than 500,000 for critical components. Their identification should provide further insight into the signals triggering this morphogenetic alteration, as well as into the effector mechanism.

Acknowledgments

Literature Cited

Amende, L. M., and S. K. Pierce. 1980a. Cellular volume regulation in salinity stressed mollusks: the response of Noetia ponderosa (Arcidae) red blood cells to osmotic variation. J. Comp. Physiol. 138: 283–289.

Amende, L. M., and S. K. Pierce. 1980b. Free amino acid mediated volume regulation of isolated Noetia ponderosa red cells: control by Ca2+ and ATP. J. Comp. Physiol. 138: 291–298.

Bang, F. B. 1961. Reaction to injury in the oyster (Crassostrea virginica). Biol. Bull. 121: 57–68.

Bergner A., T. Muta, S. Iwanaga, H. G. Beisel, R. Delotto, and W. Bode. 1997. Horseshoe crab coagulogen is an invertebrate protein with a nerve growth factor-like domain. Biol. Chem. 378: 283–287.

Bradford, M. M. 1976. A rapid and sensitive method for the quantitation of microgram quantities of protein utilizing the principle of protein-dye binding. Anal. Biochem. 72: 248–254.

Cohen, W. D. 1991. The cytoskeletal system of nucleated erythrocytes. Int. Rev. Cytol. 130: 37–83.

Cohen, W. D., ed. 1997. Compendium of Physiological Solutions. Biol. Bull. Comp. [Online] Biological Bulletin Publications, Marine Biological Laboratory, Woods Hole, MA. Available: http://www.mbl.edu/html/BB/COMPENDIUM/Comp-TabCont.html. [1999, April 12].

Cohen, W. D., and I. Nemhauser. 1980. Association of centrioles with the marginal band of a molluscan erythrocyte. J. Cell. Biol. 86: 286–291.

Cohen, W. D., and I. Nemhauser. 1985. Marginal bands and the cytoskeleton in blood cells of marine invertebrates. Pp. 1–49 in Blood Cells of Marine Invertebrates. W. D. Cohen, ed. Alan R. Liss, New York.

Cohen, W. D., P. B. Armstrong, J. Levin, R. L. Ornberg, I. Nemhauser, K. T. Edds, N. B. Terwilliger, R. C. Terwilliger, and S. K. Pierce. 1985. Blood cells of marine invertebrates: a practical guide. Pp. 251–279 in Blood Cells of Marine Invertebrates, W. D. Cohen, ed. Alan R. Liss, New York.

Dadacay, A-V. M., J. C. Huerta, C. J. Theiner, S. Swarnakar, and W. D. Cohen. 1996. Reversible alteration of molluscan erythrocyte morphology by a natural hemolymph activity. Biol. Bull. 191: 276–277.

der Terrossian, E., C. Deprette, I. Lehbar, and R. Cassoly. 1994. Purification and characterization of erythrocyte caldesmon. Hypothesis for an actin-linked regulation of a contractile activity in the red blood cell membrane. Eur. J. Biochem. 219: 503–511.

Feng, S. Y. 1965. Heart rate and leucocyte circulation in Crassostrea virginica. (Gmelin). Biol. Bull. 128: 198–210.

Feng, S. Y. 1988. Cellular defense mechanisms of oysters and mussels. Am. Fish. Soc. Spec. Publ. 18: 153–168.

Forer, A., and O. Behnke. 1972. An actin-like component in spermatocytes of a crane fly (Nephrotoma suturalis Loew). I. The spindle. Chromosoma 39: 145–173.

Fowler, V. M. 1986. An actomyosin contractile mechanism for erythrocyte shape transformations. J. Cell. Biochem. 31: 1–9.

Fowler, V. M., J. Q. Davis, and V. Bennett. 1985. Human erythrocyte myosin: identification and purification. J. Cell Biol. 100: 47–55.

Joseph-Silverstein, J., and W. D. Cohen. 1984. The cytoskeletal system of nucleated erythrocytes. III. Marginal band function in mature cells. J. Cell. Biol. 98: 2118–2125.

Joseph-Silverstein, J., and W. D. Cohen. 1985. Role of the marginal band in an invertebrate erythrocyte: evidence for a universal mechanical function. Can. J. Biochem. Cell Biol. 63: 621–630.

Lee, K. G., N. Mohan, Z. Koroleva, L-F. Huang, and W. D. Cohen. 1998. Fluorescence localization of cytoskeletal proteins in fibrin-trapped cells. Biol. Bull. 195: 211–212.

Nemhauser, I., J. Joseph-Silverstein, and W. D. Cohen. 1983. Centrioles as microtubule organizing centers for marginal bands of molluscan erythrocytes. J. Cell. Biol. 96: 979–989.

Pasternack, G. R., and R. H. Racusen. 1989. Erythrocyte protein 4.1 binds and regulates myosin. Proc. Natl. Acad. Sci. U.S.A. 186: 9712–9716.

Pierce, S. K., and T. Maugel. 1985. A comparison of the water-regulating responses of bivalve and polychaete red cells to osmotic stresses. Pp. 167–189 in Blood Cells of Marine Invertebrates. W. D. Cohen, ed. Alan R. Liss, New York.

Pierce, S. K., A. D. Politis, D. H. Cronkite, L. M. Rowland, and

L. H. Smith, Jr. 1989. Evidence of calmodulin involvement in cell volume recovery following hypo-osmotic stress. *Cell Calcium.* **10:** 159–169.

Ratcliffe, N. A., and A. F. Rowley, eds. 1981. *Invertebrate Blood Cells,* Vols. 1 and 2. Academic Press, London.

Sparks, A. K., and J. F. Morado. 1988. Inflammation and wound repair in bivalve molluscs. *Am. Fish. Soc. Spec. Pub.* **18:** 139–152.

Sullivan, G. E. 1961. Functional morphology, microanatomy, and histology of the "Sydney cockle," *Anadara trapezia* (Deshayes) (Lamellibranchia: Arcidae). *Aust. J. Zool.* **9:** 219–257.

Terwilliger, N. B., R. C. Terwilliger, and E. Schabtach. 1985. Intracellular respiratory proteins of sipuncula, echiura, and annelida. Pp. 193–225 in *Blood Cells of Marine Invertebrates.* W. D. Cohen, ed. Alan R. Liss, New York.